

The east–west effect for atmospheric neutrinos

Paolo Lipari

Dipartimento di Fisica, Università di Roma “la Sapienza”,
and I.N.F.N., Sezione di Roma, P. A. Moro 2,
I-00185 Roma, Italy

also at: Research Center for Cosmic Neutrinos,
ICRR, University of Tokyo
Midori-cho 3-2-1, Tanashi-shi, Tokyo 188-8502, Japan

March 2, 2000

Abstract

The atmospheric neutrino fluxes observed by underground detectors are not symmetric for rotations around the vertical axis. The flux is largest (smallest) for the ν 's traveling toward east (west). This asymmetry is the result of the effects of the geomagnetic field on the primary cosmic rays and on their showers. The size of the asymmetry is to a good approximation independent from the existence of neutrino oscillations, and can in principle be predicted without any ambiguity due to existence of unknown new physics. We show that there is an interesting hint of discrepancy between the experimental measurement of the east–west asymmetry by Super–Kamiokande and the existing theoretical predictions. We argue that the discrepancy is a real effect caused by the neglect, in the existing calculations, of the bending of the charged secondary particles (in particular of the muons) in the cosmic ray showers. The inclusion of this effect in the calculation gives results in quantitative agreement with the data. We comment on the implications of this result for the study of neutrino oscillations.

1 Introduction

The precise calculation of the fluxes of atmospheric neutrinos has become a much more interesting task since the measurements of Super–Kamiokande [1] and other detectors [2, 3, 4, 5] have given convincing evidence that ν flavor transitions exist and are modifying the intensity and distorting the angular distributions of the ν fluxes. As the field of atmospheric neutrino is maturing from the “discovery era” to the era of “precision measurements” the need for detailed, accurate predictions for the the atmospheric neutrino fluxes has clearly grown in importance, since comparison of data and predictions is now used to extract from the data the parameters that describe exciting new physics. At the same time the task of calculating the expected fluxes is now more demanding, since errors in the calculation, or the use of flawed data as input can result in the introduction of biases in the estimate of these parameters.

The study of the zenith angle distributions of the neutrino fluxes is obviously of central importance in the determination of the oscillation parameters. The neutrino pathlength L

(and the density profile encountered by a neutrino during its path) are strictly correlated with the zenith angle θ_ν (the correlation is not perfect because the neutrino creation point along the straight line defined by its momentum at detection is not exactly known). The neutrino flavor transition probabilities depend on the pathlength L (or more in general on the neutrino path), and therefore leave their imprints on the zenith angle distributions.

The azimuth angle distributions are much less interesting. The only significant source of non-flatness for these distributions are the effects of the geomagnetic field. In fact, neglecting the existence of the magnetic field, the geometry of the neutrino source volume (a spherical shell of air) and of the volume where neutrinos propagate, with very good approximation have cylindrical symmetry for rotations around the vertical axis¹. Neutrino oscillations (or in fact any other forms of transition or disappearance proposed as an explanation for the atmospheric ν data) do not disturb this symmetry². The fact that the azimuth angle distributions are independent from the new physics that is investigated, has however a positive consequence, their study can provide an important cross check for the theoretical predictions and the experiments. The calculations must be able to predict the shape of these distributions, without the need of additional (unknown) physics beyond the standard model, and experiments must be able to measure angular effects that are unambiguously predicted.

1.1 The hint of a discrepancy between data and prediction

The fluxes of (positively charged) primary cosmic rays that reach the Earth's atmosphere contain more particles traveling from west toward east than in the opposite direction. The discovery of this effect in 1933 [6, 7] allowed to determine that the dominant component of the cosmic rays is positively charged. This “primary asymmetry” is also reflected in the intensity of the fluxes of secondary particles that are generated in the showers of the primary particles and have a direction correlated with the primary one.

The Super-Kamiokande (SK) detector [8] has measured the azimuth angle distributions of atmospheric neutrinos, finding as expected that the distributions are not flat, and that there is an excess of particles traveling toward east. In the SK analysis the east-west asymmetry is defined as:

$$A = \frac{(N_E - N_W)}{(N_E + N_W)} \quad (1)$$

where N_E (N_W) is the number of events with the detected charged lepton traveling toward east (west). After selecting events with the charged lepton ($\ell = e, \mu$) in the momentum interval $p_\ell(\text{GeV}) = [0.4, 3]$ and the zenith angle region $|\cos\theta_\ell| < 0.5$, the measured asymmetries are:

$$A_e^{\text{SK}} = 0.21 \pm 0.04, \quad A_\mu^{\text{SK}} = 0.08 \pm 0.04 \quad (2)$$

This has to be compared with predictions from Honda, Kasahara, Kajita and Midorikawa

¹ Other sources of asymmetry can in principle be the presence of mountains (especially above the detector) and the existence of different profiles of the atmosphere in different geographical locations. The first effect is easily calculable. Both effects are expected to be negligibly small.

² If an east-west asymmetry is generated by some other source (for example geomagnetic effects), neutrino oscillations can in principle affect the *size* of the asymmetry, since oscillations can distort the ν energy spectrum. This effect is of second order, and a small correction to the calculated east-west asymmetry.

(HKKM) [9] and the Bartol group [10]:

$$A_e^{\text{HKKM}} = 0.13 \quad A_\mu^{\text{HKKM}} = 0.11 \quad (3)$$

$$A_e^{\text{Bartol}} = 0.17 \quad A_\mu^{\text{Bartol}} = 0.15 \quad (4)$$

Considering the statistical errors and the spread in the theoretical prediction, the SK collaboration concludes that both measured asymmetries are compatible with the expectations. However, if we consider the ratio A_e/A_μ , we can see that there is a hint (at the level of 2–2.5 standard deviations) of a discrepancy between the calculations that predict asymmetries that are approximately equal for e -like and μ -like events (with only a small excess for e -like events) and the data where A_e is events is more than twice larger than the asymmetry for μ -like events. We also note that there is an indication that the measured asymmetry for e -like events is larger than the prediction while on the contrary the prediction for μ -like events is smaller.

A discrepancy between data and calculation for the azimuthal distributions can have a non negligible importance for the interpretation of the data. The study of the east–west asymmetry probes the atmospheric neutrino fluxes in the angular region around the horizontal plane that is actually the most important one for the determination of Δm^2 . The fact that the results for e -like and μ -like events differ from the expectations, and in *opposite* directions, in a situation where ν oscillations cannot play a role, is clearly important for the studies of neutrino oscillations, where the comparison of the events rates for the two lepton types is a cornerstone of the analysis.

In this work we predict that with increasing statistics the Super–Kamiokande measurement of the east–west asymmetry will clearly show to be in disagreements with the predictions of [9] and [10], and indeed with any other prediction based on a calculation that does not take into account the effects the bending in the geomagnetic field of secondary charged particles in the cosmic ray showers (even if the calculation is three dimensional [11]). The existing calculations predict an east–west asymmetry that is simply the reflection of the asymmetry of the primary cosmic ray. In this case the asymmetries for e -like and μ -like events (and indeed for all for neutrino types $\nu_e, \bar{\nu}_e, \nu_\mu, \bar{\nu}_\mu$). As we will discuss in the following the effect of the magnetic field in the development of the shower in the atmosphere results in different asymmetries for the different neutrino types, in good agreement with the Super–Kamiokande data.

This work is organized as follows. In the next section we rapidly summarize the effects of the geomagnetic field on the primary cosmic rays. Section 3 contains a discussion of the effects of the geomagnetic field on the shower development. Section 4 discusses the effects of the bending of the muon trajectories in in the geomagnetic field. This is the key mechanism that enhances or suppresses the asymmetry for the different neutrino flavors. In section 5 we show the results of a complete calculation that includes the bending in the geomagnetic fields of all secondary charged particles. Section 6 gives a summary and some conclusions. An appendix contains a brief discussion on the difficulty of performing a detailed and accurate “three–dimensional” calculation of the atmospheric neutrino fluxes and on the possible strategies that are under study.

2 The East–West effect for the primary cosmic rays

The flux of primary cosmic rays protons and nuclei that arrive in the vicinity of the Earth surface exhibits the well known east–west effect, that is there are more particles traveling from west toward east than in the opposite direction. This is due to the effects of the geomagnetic field that forbids the lowest rigidity particles from reaching the Earth. The effect is strongest for west–ward going positively charged particles.

As an illustration let us approximate the geomagnetic field as a dipole, and study the trajectories of charged particles in the equatorial plane. The magnetic field is orthogonal to the plane, pointing “up” toward the magnetic pole in the northern hemisphere. Near the surface of the Earth the field has an approximately constant value $B \sim 0.31$ Gauss. A positively (negatively) charged particle with unit charge and momentum $p \simeq 59$ GeV can have a clockwise (counterclockwise) circular trajectory that grazes the Earth along the equator going from east to west (from west to east)³. It is clear that an observer at the equator looking near the horizon toward magnetic east (west) can only see unit charge primary particles with a momentum larger than 59 GeV, all lower momentum particles have “forbidden trajectories”. If the equatorial observer turns around by 180 degrees, he/she can see primary particles of much lower momenta. This is qualitatively the origin of the east–west effect.

The problem of calculating the geomagnetic effects on the primary cosmic rays (before they reach the atmosphere) can be reduced to the problem of calculating “allowed” and “forbidden trajectories”. The definition of allowed and forbidden trajectories is the following. Let us consider a cosmic ray of charge q , momentum \vec{p} near the Earth surface in position \vec{x} , and let us study the past trajectory of the particle. This study can have three results:

- (a) the trajectory originates from the Earth’s surface;
- (b) the trajectory remains confined in the volume $R_{\oplus} < r < \infty$ without ever reaching “infinity”;
- (c) the particle in the past was at very large distances from the Earth.

Trajectories belonging to the classes (a) and (b) are considered as “forbidden”, because no primary cosmic ray particle can reach the Earth from a large distance traveling along one of these trajectories. All other trajectories are allowed.

The algorithm (used in all calculations of the atmospheric neutrino fluxes) to obtain the primary cosmic ray fluxes as a function of position and angle is based on two steps:

1. It is assumed that the primary cosmic rays at a distance of one astronomical unit from the sun are isotropic, unless they are disturbed by the presence of the Earth.
2. The flux arriving at an imaginary surface in the vicinity of the Earth (the “top of the atmosphere”) is equal to the isotropic primary flux after the subtraction of all “forbidden trajectories”.

³The trajectory is unstable even in the case of an exactly dipolar field

The theoretical basis for the “subtraction algorithm” is solidly motivated [12], and is based on two fundamental assumptions, that the cosmic ray spectrum “in the absence of the Earth” is isotropic, and that the field around the Earth is well described by a static purely magnetic field. The Liouville theorem states that the density of points in phase space volume is constant. The flux $\phi(\vec{p}, \vec{x})$ is in fact proportional to the phase space density for relativistic particles, and since the momentum of a charged particle in a magnetic field is constant, then the differential flux $\phi(\vec{p}, \vec{x}(t))$ along a particle trajectory is constant. It follows that if the flux is isotropic at large distances from the Earth, then the flux in a small cone around any trajectory is constant and independent from the position. If a particle can reach the Earth, then the momentum spectrum, and the angular distribution around it are not deformed.

For the explicit calculation of allowed and forbidden trajectories, the most accurate method is the so called “back-tracking method” that is a straightforward direct application of the definition outlined above. Given a detailed map of the magnetic field around the Earth (for example see [13]) it is a straightforward exercise to compute numerically the past trajectories of a cosmic ray from a point “just above” the atmosphere, and test if it corresponds to an allowed or forbidden trajectory.

It is well known that the problem of calculating allowed and forbidden trajectories can be solved analytically for the special case of a volume that is entirely filled with an exactly dipolar magnetic field (there are no class (a) trajectories in this model). In this case the geomagnetic effects result in a sharp rigidity cutoff⁴. For a given position \vec{x} and a given direction \hat{n} the trajectories of all positively (negatively) particles with rigidity $R > R_S^+$ ($R < R_S^-$) are allowed and the trajectories of all particles with $R < R_S^+$ ($R > R_S^-$) are forbidden because they remain confined to a finite distance from the dipole center. The quantity $R_S^\pm(\vec{x}, \hat{n})$ is the Störmer rigidity cutoff [14]:

$$R_S^+(r, \lambda_M, \theta, \varphi) = \left(\frac{M}{2r^2} \right) \left\{ \frac{\cos^4 \lambda_M}{[1 + (1 - \cos^3 \lambda_M \sin \theta \sin \varphi)^{1/2}]^2} \right\} \quad (5)$$

where we have made use of the cylindrical symmetry of the problem, M is the magnetic dipole moment of field, r is the distance from the dipole, λ_M the magnetic latitude, θ the zenith angle and φ an azimuth angle measured clockwise from magnetic north. The Störmer cutoff has been of considerable historical importance. It is not sufficiently accurate for a modern detailed numerical study. but it remains a good approximation that contains all qualitative features of an “exact” numerical calculation, and remains a very valuable tool to gain physical insight and qualitative understanding. We can use it to illustrate the three most important qualitative points that we will need for the discussion in this work.

1. The geomagnetic effects depend on the detector position. They are strongest near the equator and weakest at the magnetic poles. In equation (5) we can see that the value of the cutoff grows monotonically from a vanishing value at the magnetic pole ($\lambda_M = \pm 90^\circ$) to a maximum value at the magnetic equator ($\lambda_M = 0^\circ$).

⁴In a numerical calculation for a non exactly dipolar field, or even in the case of a dipole, if the trajectories that have a segment inside the Earth are also considered as forbidden, there is not anymore a sharp cutoff, but in a narrow interval allowed and forbidden bands of rigidity alternate.

2. The set of allowed rigidities is largest for particles traveling toward magnetic east. In equation (5) for a fixed detector position (fixed λ_M) and a fixed zenith angle θ , the cutoff is minimum (maximum) for azimuth angle $\varphi = 270^\circ$ ($\varphi = 90^\circ$) that corresponds to a particle traveling toward east (west).
3. For a fixed detector position and a fixed azimuth angle the set of allowed rigidities is largest (smallest) for vertical (horizontal) particles. In equation (5) for λ_M and φ fixed, the cutoff grows monotonically with θ .

The east–west asymmetry of the primary cosmic ray radiation is of course reflected in asymmetries for the fluxes of secondary particles generated in their showers in the atmosphere. This effect results in asymmetries of approximately the same size for all four neutrino types. This is a consequence of the fact that a primary particle of energy E_0 produces yields of ν_e , $\bar{\nu}_e$, ν_μ and $\bar{\nu}_\mu$ with approximately the same energy spectrum (and relative normalizations in the ratios 1 : 1 : 2 : 2). The existing calculations of the neutrino fluxes only include the geomagnetic effects on the the primary flux as a source of an azimuthal asymmetry and as a consequence the predicted east–west neutrino asymmetries are all of approximately the same size.

3 Effects of the geomagnetic field on the shower development

3.1 Bending of the trajectories of charged particles

The trajectories of all charged particles in cosmic rays showers are curved because of the presence of the geomagnetic field. It will be particularly important in this work to consider the effect of the bending on the zenith angle of the particles, that is to study if the particle trajectories are bent “upward” or “downward”. We can define a (position dependent) system of coordinates with the z axis pointing up, the x axis pointing toward magnetic north and the y axis completing a right–handed system pointing toward the magnetic west. In this system the magnetic field has by definition components $\vec{B} \equiv (|B_{\text{hor}}|, 0, B_{\text{vert}})$ with B_{vert} positive (negative) in the southern (northern) hemisphere. The equation of motion of a charged particle in the geomagnetic field for the vertical component is:

$$\frac{dp_z}{dt} = -q \beta_y |B_{\text{hor}}| = +q \beta_{\text{east}} |B_{\text{hor}}|, \quad (6)$$

where q is the electric charge and $\vec{\beta}$ the velocity of the particle. Positively charged particles ($q > 0$) traveling east ($\beta_y < 0$) have $dp_z/dt > 0$, and are bent up. Negatively charged particles with the same initial direction are bent down. The reverse happens for particle traveling in the opposite (west–ward) direction ($\beta_y > 0$): negatively charged particles are bent up while positively charged ones are bent down.

An example of the bending of charged particles is shown in fig. 1. The figure is in true scale and represents a projection of the space above the Super–Kamiokande detector. The center of the SK detector (latitude 36.42° N, longitude 137.31° E, and altitude 371.8 meters above sea level [8]) corresponds in the figure to the point with coordinates (0,0.3718). The thick line represents the “sea level” surface of the Earth in the vicinity of SK detector.

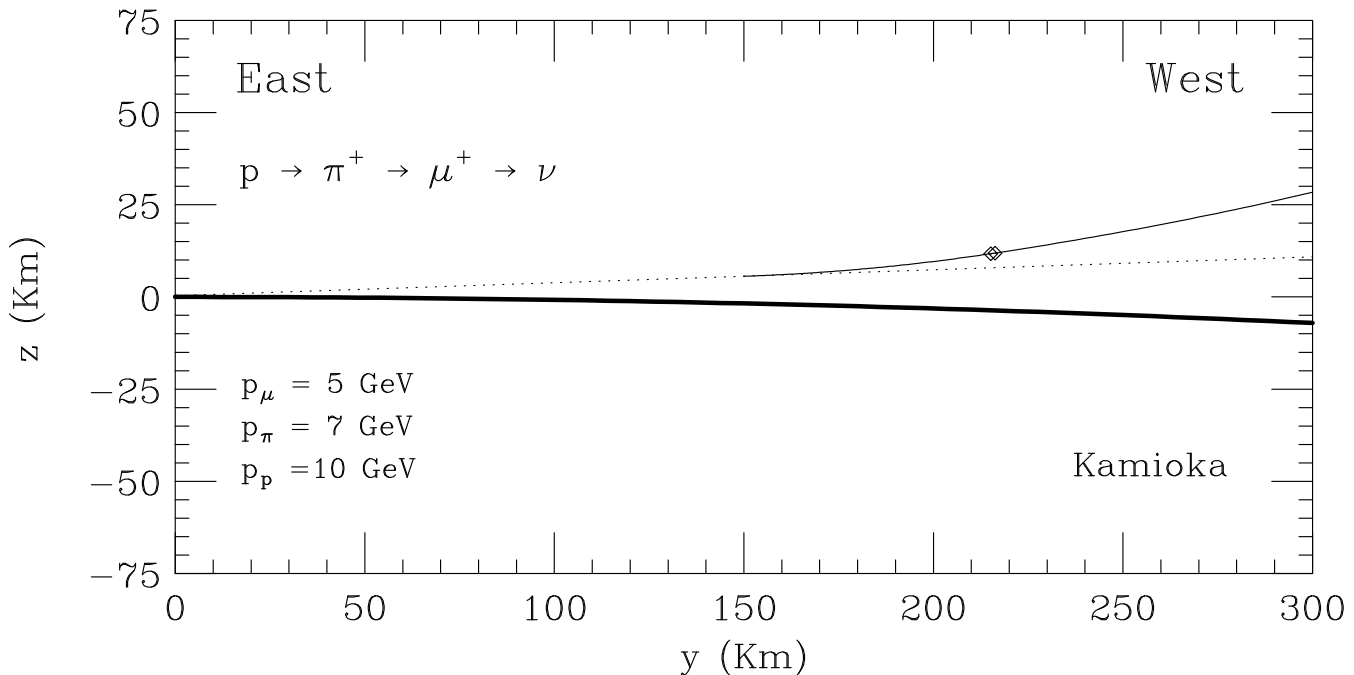


Figure 1: Deviation of a muon in the geomagnetic field above the SK detector (see text).

The z axis corresponds to the vertical axis that passes through the SK center, and the horizontal axis points to geographical west. The thin solid lines describe the projections in the plane of the figure of the trajectories of three charged particles. The particles are part of a cosmic ray shower and are “connected” by a production chain $p \rightarrow \pi^+ \rightarrow \mu^+$. The trajectories are calculated integrating the equations of motion for charged particles in the International Geomagnetic Reference Field (IGRF [13]) for the year 2000 and correspond to a 10 GeV proton, a 7 GeV π^+ and a 5 GeV μ^+ . The pion production and decay points are marked by two diamonds. The muon emits a neutrino (the trajectory and its continuation beyond is indicated by a dotted line) that intersects the SK detector. For illustration both the pion and the muon decay after exactly three proper lifetimes. Both the pion and the muon are emitted exactly collinearly with respect to the primary (or parent) particle, so the angle between the neutrino and the primary directions is entirely due to the effects of the geomagnetic field. Since all three particles are positive and travel toward the east direction they are bent upward.

In the following we will study the effects of the bending of the shower particles in the magnetic field on the fluxes of atmospheric neutrinos. These effects have been ignored in all previous calculations. In our numerical work we have included the bending of all charged particles in the shower. In the qualitative discussion that follows we will discuss separately the effect of the bending on the primary particles, and on the muons produced in the showers. These are in fact the most important sources of the effects we have found. Charged pions have a lifetime that is two orders of magnitude shorter than τ_μ (and a mass similar to m_μ), therefore their bending in the magnetic field is much less important than for muons. Most of the neutrinos are produced in the chain decay of mesons produced

in the first interaction of a primary. Also for those produced deeper in the shower most of the interesting effects is the result of the bending of the primary particles and the muons.

Note that we can expect that the effects of the field will be especially important for the neutrinos that come from muon decay, and significantly smaller for the muon (anti)–neutrinos produced directly in meson decay.

3.2 The bending of the primary particles

It is incorrect to think that all effects of the magnetic field on the primary particles are taken into account by the study of allowed and forbidden trajectories discussed in section 2. The bending of the primary particles is a factor in determining the average altitude of the primary interactions, and the zenith angle distribution of the primaries at the interaction point. These two effects are not taken into account in the existing calculations. Note that the zenith angle (that is the polar angle with respect the local vertical) of a particle can be calculated as:

$$\cos \theta = -\frac{\vec{p} \cdot \vec{r}}{|\vec{p}| |\vec{r}|} \quad (7)$$

and is not a constant even for particles traveling along a straight line. The value of the zenith angle along a particle trajectory will of course be determined by the bending in the magnetic field.

As an illustration let us study the trajectories of two protons both on allowed trajectories that cross an imaginary spherical surface above the Earth with the same zenith angle but different azimuth angles, with one particle traveling toward east, and second one toward west. If the two trajectories are approximated as straight lines the distributions of altitude of the interaction point for the two particles (determined by the interaction length λ_{int} , the inclination of the trajectory and the altitude profile of the air density) will of course be identical. It is however easy to see that since the east–going particle is bent “up”, and the west–going one is bent “down”, the first particle will on average interact higher, and more “horizontally”:

$$\langle h_{\text{int}} \rangle_E > \langle h_{\text{int}} \rangle_W, \quad (8)$$

$$\langle \cos \theta_0^{\text{int}} \rangle_E < \langle \cos \theta_0^{\text{int}} \rangle_W \quad (9)$$

Both the inequalities (8) and (9) result in an enhancement of the east–west effect for the neutrinos. The average number of neutrinos produced in a shower is larger when the primary particle interacts higher because the muons have a longer pathlength for decay, and the shower develops in a medium of lower density where the decays of mesons is enhanced, and muons lose less energy before decay. For the same reasons more inclined showers produce more neutrinos.

In summary we can expect that the bending of the primary particle inside the atmosphere result in an enhancement of the neutrino east–west asymmetry with respect to the estimates that only consider the bending in vacuum. This enhancement will be approximately equal for all four neutrino types, it is therefore an interesting effect, but it is cannot be the explanation for the (hint of) discrepancy between data and prediction represented by equations (2), (3) and (4).

3.3 The angle between the neutrino and the primary particle

For the effects that we want to consider it is essential to consider the difference in direction between a neutrino and the primary particle that generated the shower where it was produced. We introduce the notation: $\Omega_\nu = \Omega_0 \oplus \Omega_{0\nu}$ where Ω_ν is the direction of the detected neutrino, Ω_0 the direction of the primary particle, and $\Omega_{0\nu}$ the angle between the neutrino and the primary. The angle $\Omega_{0\nu}$ is the result of the combination of several processes. For the neutrinos that are produced directly in a meson decay we can write:

$$\Omega_{0\nu} = \Omega_{0\pi} \oplus \Omega_{\pi\nu} \quad (10)$$

where $\Omega_{0\pi}$ the direction of emission of the parent pion in the primary interaction, and $\Omega_{\pi\nu}$ the direction of emission of the neutrino in the pion decay (this qualitative discussion obviously applies also for kaons). Similarly for neutrinos emitted in the chain decay $\pi \rightarrow \mu\nu$ we have:

$$\Omega_{0\nu} = \Omega_{0\pi} \oplus \Omega_{\pi\mu} \oplus \Omega_{\mu B} \oplus \Omega_{\mu\nu} \quad (11)$$

where $\Omega_{\pi\mu}$ ($\Omega_{\mu\nu}$) is the emission direction of the muon (neutrino) in the decay of the pion (muon), and $\Omega_{\mu B}$ is the deviation of the muon in the geomagnetic field (the deviations in the magnetic field of the other charged particles are typically two orders of magnitude smaller; they are included in our numerical work).

The average deviation (considered as a space angle) α_j for the process j can be easily estimated in first order:

$$\alpha_{0\pi} \sim \frac{\langle p_\perp \rangle_\pi}{p_\pi} \sim \frac{4\langle p_\perp \rangle_\pi}{p_\nu} \sim \frac{5.2^\circ}{p_\nu(\text{GeV})}, \quad (12)$$

where we have used the approximation $p_\pi \sim 4p_\nu$ (since a charged pion energy is approximately shared equally between three neutrinos and a e^\pm) and have assumed a transverse momentum $\langle p_\perp \rangle \sim 350$ MeV;

$$\alpha_{\pi\nu} \sim \frac{p^*}{p_\nu} \sim \frac{1.7^\circ}{p_\nu(\text{GeV})} \quad (13)$$

where p^* is the center of mass momentum of the final state particles in the decay $\pi \rightarrow \mu\nu$;

$$\alpha_{\pi\mu} \sim \frac{p^*}{p_\mu} \sim \frac{3p^*}{p_\nu} \sim \frac{0.6^\circ}{p_\nu(\text{GeV})} \quad (14)$$

this is approximately 3 times smaller than (13) because the muons have on average three times the energy of their neutrino decay products;

$$\alpha_{\mu\nu} \sim \frac{m_\mu/3}{p_\nu} \sim \frac{2.0^\circ}{p_\nu(\text{GeV})} \quad (15)$$

and for the deviation of the muons in the magnetic field:

$$\alpha_{\mu B} \sim \frac{L_\mu}{R_\mu} \simeq \left(\tau_\mu \frac{p_\mu}{m_\mu} \right) \left(\frac{eB}{p_\mu} \right) \sim 10.7^\circ B(\text{Gauss}) \quad (16)$$

where L_μ is the muon decay length, R_μ the muon gyro-radius in the geomagnetic field, and B the value of the field. In this estimate we have neglected the muon energy loss and we have also assumed that the muons decay before hitting the ground.

There are two fundamental differences between the effect of the magnetic bending and the other contributions to $\Omega_{0\nu}$. The first difference is that all deviations, except the magnetic bending one scale $\propto p_\nu^{-1}$ reflecting the forward boost in the interaction or decay of relativistic particles. The deviation of the muons in the geomagnetic field is (in first order) independent from the muon momentum, because both the magnetic rigidity and the decay pathlength increase proportionally to p_μ . Higher momentum muon bend less in the field, but live longer and the field can act for a longer time.

The second and most important difference is that all deviations (except the bending one) are azimuthally symmetric, therefore if we consider the deviation in any plane, the average value vanishes. The deviation in the magnetic field is of course not an “average value”, all muon of the same initial momentum have exactly the same deviation, and the deviation is not azimuthally symmetric but happens in a well defined plane. If we for example consider the average zenith angle of the neutrinos produced in the showers generated by primaries of fixed direction $\Omega_0 \equiv (\cos \theta_0, \varphi)$ we find that the average contribution of all sources vanishes, except for the effect of the bending in the field.

$$\langle \theta_\nu \rangle = \theta_0 + \langle \theta_{\mu B} \rangle \quad (17)$$

This effect plays a crucial role in determining the neutrino east–west asymmetry.

4 Magnetic bending of μ^\pm and the ν east–west asymmetries

The effect of the geomagnetic field on the trajectory of charged particles (equation (6)) implies (a scheme of the results is also shown in fig. 2):

- (a) Positively charged particle ($q > 0$) traveling toward east ($\beta_y < 0$) are bent “up”.
- (b) Positively charged particle ($q > 0$) traveling toward west ($\beta_y > 0$) are bent “down”.
- (c) Negatively charged particle ($q < 0$) traveling toward east ($\beta_y < 0$) are bent “down”.
- (d) Negatively charged particle ($q < 0$) traveling toward west ($\beta_y > 0$) are bent “up”.

From equation (17) we can then deduce that neutrinos produced in the decay of positive (negative) muons in showers of east–ward (west–ward) traveling primaries will be on average more “horizontal” than the primary particle; conversely the neutrinos produced in the decay of positive (negative) muons in showers of west–ward (east–ward) traveling primaries will be on average more “vertical” than the primary particle.

The key remark is now, that this systematic difference between the zenith angle of the neutrino and the primary results for the cases (a) and (d) in an enhancement and for the cases (b) and (c) in a suppression of the neutrino flux.

Two effects play a role in the enhancement or suppression of the flux. The first effect is purely geometrical and would be present even for an exactly isotropic primary flux (this is not so academic as it may sound, because the primary flux *is* actually isotropic for all

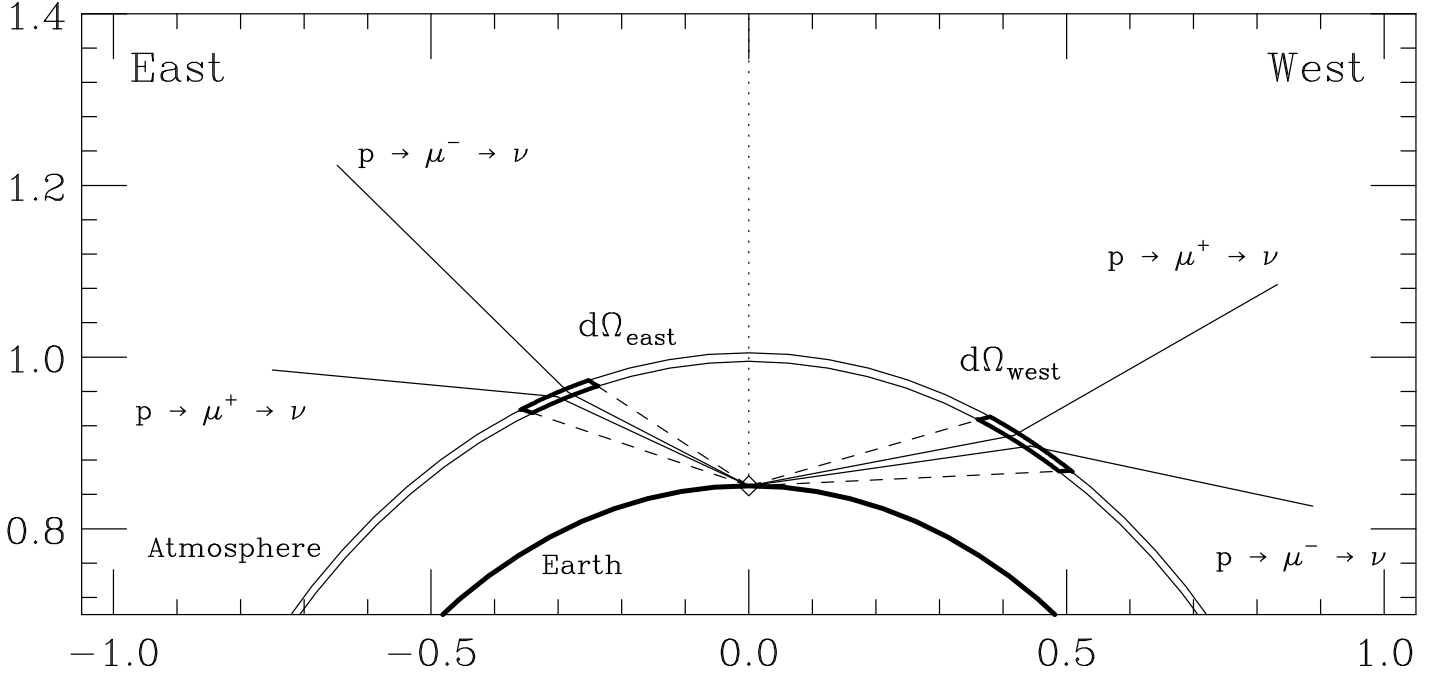


Figure 2: Relation between the directions of the primary particle and of the detected neutrinos, for ν 's produced in muon decay (see text).

rigidities above 60 GV). In this case the rate of primary interactions with zenith angle θ_0 is $\propto \cos \theta_0$, and there is an excess of vertical showers over horizontal ones. Therefore if the zenith angle of the primary particles is smaller (larger) than the neutrino one we can expect a larger (smaller) event rate. This is illustrated schematically in the diagram of fig. 2. The neutrinos detected by an observer (indicated by a diamond) located on the surface of the Earth (shown as a thick line) looking in the solid angle $d\Omega_{\text{west}}$ (indicated by a dashed cone) are produced in a “patch” (outlined with a thick line) of atmosphere (that in the diagram is represented by a thin spherical shell) subtended by the solid angle $d\Omega$. It can be seen from the figure that this patch of atmosphere “looks” larger (it has a larger projected area) for the primary particles if the production chain is $p \rightarrow \pi^+ \rightarrow \mu^+ \rightarrow \nu$ (the neutrinos can be ν_e and $\bar{\nu}_\mu$) than in the case when the neutrinos are produced directly in meson decay. This is a simple consequence of the fact that the projected area of the element of atmosphere subtended by the solid angle $d\Omega$ is proportional to $\cos \theta_0$. For a fixed neutrino zenith angle, the average value of the primary zenith angle is not a constant but depends on the production mechanism. In the case $p \rightarrow \pi^+ \rightarrow \mu^+ \rightarrow \nu$ the relation between the zenith angle of the primary and of the neutrinos is $\langle \theta_\nu \rangle < \theta_0$, in the case of neutrinos directly from meson decay: $\langle \theta_\nu \rangle \simeq \theta_0$. Similarly the patch of atmosphere “looks” smaller for the primaries when the production process is $p \rightarrow \pi^- \rightarrow \mu^- \rightarrow \nu$ (the neutrinos are $\bar{\nu}_e$ and ν_μ) since in this case the relation between the zenith angle of the neutrinos and the primary is: $\langle \theta_\nu \rangle > \theta_0$. The bending in different directions of positive and negative muons results in one case in an enhancement, and in the other in a suppression of the neutrino fluxes. This discussion can be repeated for a solid angle

$d\Omega_{\text{east}}$ in the opposite hemisphere, with the crucial difference that the production chains that are enhanced and suppressed are interchanged.

If now we consider the fact that the primary cosmic rays that reach the Earth's atmosphere are not isotropic we find actually that the enhancement and suppression are *stronger* than what is obtained with the geometrical argument outlined above. This can be understood noting that the set of forbidden trajectories becomes larger when the zenith angle increases. This can be easily seen from the Störmer formula (5) where for fixed λ_M and φ the rigidity cutoff grows monotonically with the zenith angle θ .

In summary: the effect of the magnetic bending of the muons results in an enhancement for the flux of the neutrinos produced in the decay of μ^+ (that is ν_e and $\bar{\nu}_\mu$) when the particles travel toward east, and a suppression when the particles travel toward west. The net effect is a *positive* contribution to the east–west asymmetry. The effect of magnetic bending is obviously opposite for the flux of neutrinos produced in the decay of μ^- ($\bar{\nu}_e$ and ν_μ). The flux is suppressed when the particles travel toward east, and enhanced when the particles travel toward west. The net effect is a *negative* contribution to the east–west asymmetry.

The effect of the magnetic bending of the muons has to be combined with the asymmetry generated by the geomagnetic effects on the primary particles, that to a good approximation result in an equal contribution to the asymmetry of all neutrino types. Moreover, for the neutrinos produced directly in meson decay, the effects of the geomagnetic field during the development of the shower are negligible, and for them the only significant source of asymmetry are the geomagnetic effects on the primary trajectory.

4.1 Qualitative predictions

We can finally put all results together and give some simple, non-trivial and testable predictions.

1. With increasing statistics, the Super-Kamiokande detector will detect east–west asymmetries that are *not* in agreement with predictions based on one–dimensional calculations.
2. The asymmetries for the four neutrino types are in the relation:

$$A_{\bar{\nu}_e} < A_{\nu_\mu} < A_\nu^{\text{1D}} < A_{\bar{\nu}_\mu} < A_{\nu_e} \quad (18)$$

where A_ν^{1D} is the asymmetry predicted in a one–dimensional approximation, that is approximately equal for all neutrino types.

3. The neutrino type with the largest asymmetry is the ν_e . The majority of these neutrinos are produced in the chain decay $p \rightarrow \pi^+ \rightarrow \mu^+ \rightarrow \nu_e$, and for all these neutrinos the contributions of the geomagnetic effects on the primary particle and on the muon add to each other.
4. The east–west asymmetry for $\bar{\nu}_\mu$ is smaller than for A_{ν_e} but larger than the 1–D prediction. This is a consequence of the fact that approximately one half of the $\bar{\nu}_\mu$'s are produced in μ^+ and have a large asymmetry (approximately equal to A_{ν_e}) and for

these neutrinos the geomagnetic effects on the primary particles and on the muons add to each other. The other half of the $\bar{\nu}_\mu$'s is produced in pion decay, and will have an asymmetry close to what is predicted in the 1-D approximation.

5. Developing a similar argument we can conclude that the asymmetry for ν_μ 's will be smaller than the 1-D prediction, because for approximately half of these neutrinos (those produced in the chain decay $p \rightarrow \pi^- \rightarrow \mu^- \rightarrow \nu_\mu$) the effects of the bending of the muons gives a negative contribution to the asymmetry.
6. The asymmetry for $\bar{\nu}_e$ will be the smallest one since most of the particles are produced in the decay of negative muons, and for nearly all $\bar{\nu}_e$'s the effect of the bending of the muons must be subtracted from the asymmetry generated by geomagnetic effects on the primary particles. Numerically we actually will find a *deficit* of east-going $\bar{\nu}_e$'s, that is an asymmetry that has changed sign. The effect of the muon bending overcompensates for the effect of the primary flux.
7. Even if the detector is not capable to distinguish neutrinos from anti-neutrinos, the effect of the magnetic bending of the muons is still measurable. For e -like events the net effect is an enhancement of the asymmetry with respect to the 1-D expectation:

$$A_e > A_e^{1D} \quad (19)$$

This can be simply deduced as a consequence of three steps: (i) the effect of muon magnetic bending on the asymmetry is positive for ν_e 's and negative for $\bar{\nu}_e$'s; (ii) in the neutrino flux the $\nu_e/\bar{\nu}_e$ ratio is approximately unity (more accurately ~ 1.2 , reflecting the π^+/π^- ratio in the final states of proton interactions); (iii) the cross section for neutrinos is larger than for anti-neutrinos.

8. With a very similar argument, we can estimate that the asymmetry of μ -like events must be smaller than the 1-D calculation:

$$A_\mu < A_\mu^{1D} \quad (20)$$

The inequality is opposite with respect to the e -like case, since the effect of the muon magnetic bending on the asymmetry is negative for neutrinos (with the larger cross section) and positive for anti-neutrinos.

5 Numerical results from a full 3-D calculation

To go beyond this qualitative discussion we have performed a full three-dimensional monte-carlo calculation of the atmospheric neutrino fluxes, including the bending in the geomagnetic field of all charged particles in the cosmic ray showers. This monte-carlo calculation has been already described in [17], where it was used to illustrate effects of a three-dimensional calculation on the predicted zenith angle distributions of e -like and μ -like events. We refer to [17] for more details on the calculation method, here we will only briefly summarize the main points. We have used a straightforward, direct method (see the appendix for a comparison with other approaches). The first step of the calculation is the generation of isotropic fluxes of cosmic rays (we used the results of [18]

for the energy spectrum and mass composition) at “the top of the atmosphere” (at a radius $R = R_{\oplus} + 80$ Km). The geomagnetic effects on the primary flux are computed studying the past trajectories of each generated particle. Primary particles on forbidden trajectories are rejected. Primary particles on allowed trajectories are propagated in the magnetic field (the International Geomagnetic Reference Field for the year 2000 [13]). About 97% of the particles interact in the air (the remaining fraction only grazes the Earth and continues its travel). The air is described as having a spherically symmetric distribution $\rho(r)$ obtained from a fit to the US standard atmosphere. The final states of the hadronic interactions was generated using the model (and montecarlo algorithms) of Hillas [15]. All secondary charged particles are propagated along curved trajectories in the magnetic field, and a shower is generated developing a “tree” with a standard technique. For the propagation of muons we have included the (crucially important) energy loss for ionization in the air (and the trajectory correctly takes into account the variation of the muon momentum). Energy loss was neglected for all other particles. Multiple scattering was neglected for all particles. When neutrinos are produced their trajectories (simple straight lines) are studied. Each neutrino either “misses” the Earth, or crosses its surface twice, first as down-going and then as up-going. At each intersection its position and direction of the neutrinos is recorded. To compute the azimuth of the neutrinos, for each point on the surface of the Earth we have defined a “local” system of coordinates as discussed in section 3: the z axis points up, the x axis toward magnetic “north”, and the y axis toward magnetic “west”. In this system the magnetic field has components $(|B_{\text{hor}}|, 0, B_{\text{vert}})$. The azimuth φ (following the SK convention) is defined as the direction where the particle is going: a particle with $\varphi = 90^\circ$ (270°) is traveling from east toward west (from west toward east).

The neutrinos generated with these algorithms are distributed over the entire surface of the Earth, with important non-uniformities due to the effects of the magnetic field. We have collected the neutrinos in five different regions of equal area selected according to the magnetic latitude: an equatorial region, two intermediate and two polar regions. The results in the two (north and south) polar regions and the two intermediate regions are essentially undistinguishable, and here we present only the results for the northern regions.

Our results on the azimuth distributions are collected in 6 figures (from fig. 3 to fig. 8). In the figures we plot the azimuth distribution of the event rates, obtained after the convolution of the calculated fluxes with the model of the neutrino cross section from [16]. We have selected neutrinos in the momentum interval: $p_\nu(\text{GeV}) = [0.5, 3]$ and the zenith angle region $\cos\theta_\nu = [-0.5, 0.5]$. No detection efficiency or experimental smearing has been included. For each of the three regions of the Earth that we have considered, we include two figures. The first figure contains (in four separate panels) the azimuth distributions of the four neutrino types. The second figure (in two separate panels) contains the azimuth distribution of e -like and μ -like events (these distributions are obtained simply summing together the results for ν_e and $\bar{\nu}_e$ (or ν_μ and $\bar{\nu}_\mu$). The scale of the y axis is absolute for all figures.

We have also performed the montecarlo calculation three times.

- (i) A first calculation (represented by thick histograms) was performed using the “full

3-D” algorithms described above, including the bending of all secondary charged particles in the showers.

- (ii) A second calculation (represented by thin histograms) was performed to reproduce the 1-D algorithms. The geomagnetic effects are calculated for the primary cosmic ray particles traveling outside the Earth’s atmosphere (exactly as in the previous case), but all particles travel along straight line trajectories for $r < R_{\oplus} + 80$ Km.). Also all final state particles are collinear with the projectile (or parent) particle. This is achieved modeling the interactions and particle decays exactly as in the previous case, (including therefore transverse momentum), and performing as a last step a rotation of all the 3-momenta of the final state particles so that they become parallel to the projectile (for interactions) or parent (for decays) particle.
- (iii) A third calculation (represented by dashed histograms) was performed neglecting the geomagnetic effects on the primary flux (therefore considering exactly isotropic primary fluxes) and using the 1-D algorithms outlined in the previous point. With these approximations the azimuth angle distributions *must* be flat and independent from the detector position. The only non trivial result of the calculation is the absolute normalization of the different rates. Note that this normalization must also be independent from the geographical region considered.

Inspecting the results of fig. 3 to fig. 8, we can make the following remarks.

1. Calculation (iii) (no geomagnetic effects) results as expected in flat, detector position independent azimuth distributions.
2. Calculation (ii) (1D with geomagnetic effects included for the primary) exhibits as expected an east–west asymmetry, that is of approximately the same size for all four neutrino types.
3. The taking into account of the effects of the bending in the magnetic field of secondary particles (and also of the primary in the atmosphere) in calculation (iii) is a non negligible correction.
4. Comparing the results of calculation (ii) and calculation (iii) one can see that the effects of the bending of secondary particles result in an enhancement of the east–west asymmetry for ν_e , and $\bar{\nu}_\mu$, and a suppression of the asymmetry for $\bar{\nu}_e$ and ν_μ .
5. The asymmetry for the combination $(\nu_e + \bar{\nu}_e)$ is also enhanced, while the asymmetry for the combination $(\nu_\mu + \bar{\nu}_\mu)$ is suppressed.

In summary we can observe that the expectations of the qualitative discussion of the previous section have been confirmed in a preliminary, but detailed, quantitative calculation. The results are summarized in table 1, that gives the results of the asymmetries obtained with the calculation (ii) (or 1-D) and the calculation (iii) (or 3-D), in the different geographical regions. For the definition of the magnetic latitude we have used as dipole axis the one that corresponds to the leading term in the multipole expansion of the IGRF field for the year 2000. With this definition the SK detector has a magnetic

Table 1: East–west asymmetry for different event types, after averaging for the detector position in different regions of the Earth. The events are selected with the cuts $E_\nu(\text{GeV}) = [0.5, 3]$ and $\cos\theta_\nu = [-0.5, 0.5]$. The two results are for a one–dimensional and a three-dimensional calculation that includes the bending of secondary particles in the geomagnetic field.

Region	Equatorial $\sin\lambda_M = [-0.2, 0.2]$		Intermediate $\sin\lambda_M = [0.2, 0.6]$		Polar $\sin\lambda_M = [0.6, 1]$	
	A (1D)	A (3D)	A (1D)	A (3D)	A (1D)	A (3D)
ν_e	0.194	0.431	0.126	0.335	0.026	0.214
$\bar{\nu}_e$	0.189	-0.057	0.120	-0.065	0.012	-0.061
ν_μ	0.180	0.065	0.115	0.028	0.011	0.002
$\bar{\nu}_\mu$	0.173	0.310	0.107	0.240	0.014	0.153
e	0.192	0.301	0.124	0.224	0.022	0.136
μ	0.178	0.139	0.113	0.091	0.012	0.046

latitude of 27.08° ($\sin\lambda_M^{\text{SK}} = 0.455$) and is inside the “intermediate” region in the northern hemisphere.

Inspecting table 1, we can notice that as expected the east–west asymmetry depends on the magnetic latitude of the detector, and is strongest near the magnetic equator, where all geomagnetic effects are enhanced. In the 1–D calculation the asymmetries for the four neutrino types are approximately equal, with small differences that reflect the fact that the neutrino spectra produced by a primary of fixed energy are not identical for the four flavors. The full 3–D calculation clearly exhibits the enhancements and suppressions predicted qualitatively in section 4.

6 Summary and conclusions

In this work we have shown that the azimuth angle distributions of atmospheric neutrinos are shaped by the effects of the geomagnetic field on both the trajectories of the primary cosmic rays, and their showers in the Earth’s atmosphere.

In the existing (one–dimensional) calculations of the atmospheric neutrino fluxes the effects of the magnetic field on the shower development are ignored. In a 1–D framework the asymmetries of the ν fluxes reflect only the highest suppression of the primary cosmic ray flux when the primary particles travel towards west, and the predicted east–west asymmetry is approximately equal for all four neutrino types: (ν_e , $\bar{\nu}_e$, ν_μ and $\bar{\nu}_\mu$).

The situation changes when one includes the bending in the geomagnetic field of secondary particles (and in particular of muons) in the cosmic rays showers. Positively and negatively charged particles are curved in different directions and the resulting effect on the east–west asymmetry is different for different ν types. It is an enhancement for the neutrinos that are the product of μ^+ decay (ν_e , and $\bar{\nu}_\mu$) and a suppression for the products of μ^- decay ($\bar{\nu}_e$, and ν_μ).

For detectors like Super–Kamiokande that cannot separate ν ’s and $\bar{\nu}$ ’s the detectable effect is an enhanced east–west asymmetry for the e –like events, and a suppressed asymmetry for the μ –like events, as it is already observed [8] by Super–Kamiokande. It is remarkable that the detector is able to measure successfully subtle effects as those de-

scribed here (and without the need of a prediction). In our view this is a confirmation of the high quality of the experimental data.

The (partial) failure of the existing calculations in the prediction of the east–west asymmetry is also a warning and an indication that the development of more accurate and detailed calculations of the atmospheric neutrino fluxes is needed. Several groups [19] are working in this direction. We note that a correct prediction of the east–west effects is possible only with a fully three–dimensional calculation. In our view the success of the calculation presented here in reproducing the SK results is also a confirmation of the non–trivial geometrical effects connected with 3–D effects and the geometry of the neutrino source volume discussed in [11] and in more detail in [17].

The understanding that the present calculations of atmospheric neutrinos do not describe correctly the east–west asymmetry can have some interesting consequences for the determination of the oscillation parameters from the atmospheric neutrino data (in SK and also other experiments, in particular Soudan). We note that the effects we have been discussing are obviously especially important for horizontal neutrinos, and that the effects have different sign for e –like and μ –like events. The shape of the zenith angle distribution of the atmospheric neutrino fluxes, in particular close to the horizontal plane, and the relation between the muon and electron event rates are (at least in the opinion of this author) the most important problems in the calculation of the atmospheric neutrino fluxes. As an illustration, in the simplest (and favored) picture of $\nu_\mu \leftrightarrow \nu_\tau$ oscillations for values of Δm^2 in the range indicated by the data and the range of E_ν characteristic of the contained events, the value of $\sin^2 2\theta$ can be reliably calculated comparing the “up–going” and “down–going rates”, with a relatively small systematic error and even for a poor (or even incorrect) estimate of Δm^2 . This is possible since the ratio of the rates is to a good approximation determined only the “asymptotic forms” of the oscillation probability ($P_{\nu_\mu \rightarrow \nu_\tau} = 0$ or $\sin^2 2\theta/2$) where the value of Δm^2 is absent. On the other hand the determination of Δm^2 requires a detailed fit of the zenith angle distributions, with the region close to the horizontal playing a crucial role. The (nearly exact) up–down symmetry of the ν –fluxes is of little help in this case. The comparison of the e –like and μ –like rates remains as a powerful tool to estimate the suppression (or enhancement) of a flavor type, but of course as discussed in this work, for precise quantitative evaluations of the parameters one need to study with great care the relations between the fluxes of different neutrino types.

We postpone to a future work a quantitative estimate of the effects of a full three–dimensional calculation in the determination of the allowed region in the neutrino oscillation parameter space.

Other important sources of uncertainties [20, 21] in the determination of the allowed region for the oscillation parameters are the input primary spectra, where very valuable new data became recently available [22, 23, 24], and the modeling of hadronic interactions. New data on this problem would also be of great value [25]. A detailed description of the neutrino cross section is also needed to compute the event rates, and new data would be very valuable and benefit also the long–baseline programs.

Acknowledgments Special thanks to Takaaki Kajita for very useful discussions and encouragement. I'm also grateful to Ed Kearns for discussions about the SK data, and gladly acknowledge discussions with Giuseppe Battistoni, Alfredo Ferrari, Tom Gaisser, and Yoichiro Suzuki. This work was also possible thanks to the precious help of Massimo Carboni, Kenji Kaneyuki and Atsushi Okada.

Appendix: 3-D calculations of atmospheric neutrinos

The first calculations of the atmospheric neutrino fluxes have been performed in a one-dimensional approximation, that is assuming that the neutrinos are emitted collinearly with the primary particle. This allows an enormous reduction of the size of a montecarlo calculation, because only the (formally vanishingly small) fraction of the cosmic rays showers that has trajectories that intersect the detector has to be simulated.

The difficulty of a a full three-dimensional calculation of the neutrino fluxes has been discussed in [11] and [17]. In a 3-D calculation any shower can produce a neutrino that intersect the detector we are considering, and therefore all possible showers have to be studied. Since the atmospheric neutrinos are generated quasi-uniformly over the entire surface of the Earth with a total area $5.1 \times 10^8 \text{ Km}^2$, only a very small fraction of these neutrinos will intersect a dector with an area of order 10^{-3} Km^2 . Of course it is possible to consider a detector area greatly enlarged to improve the statistical precision of the calculation, however this cannot be done arbitrarily because in fact the ν flux is not exactly uniform, but it does depend on the detector location. This in a nutshell is the computational problem of a 3-D calculation.

There are several methods that have been used or are currently under study to overcome this difficulty.

6.1 Spherically symmetric problem

A useful first step is to consider a a simpler, spherically symmetric problem, that is obtained neglecting all effects of the geomagnetic field both for the determination of allowed and forbidden trajectories, and in the development of the showers. This problem is explicitly spherically symmetric: all points on the surface of the Earth are equivalent, and the entire surface can be used as the “detector”. This calculation requires therefore the same computer power of a 1-D calculation, because essentially all produced neutrinos (all those that intersect the Earth’s surface) can be collected and analysed to “measure” the ν -fluxes in a montecarlo calculation.

A calculation along these lines has been performed by G. Battistoni et al [11]. This calculation for the first time demonstrated the existence of non-trivial geometrical effects (see [17] for more discussion) due to the spherical geometry of the neutrino source volume.

6.2 Shower translation algorithm

Unfortunately a calculation performed using the approximation of a spherically symmetric Earth is not adequate for the analysis of experimental data. The largest effect that is missing is the effect of the geomagnetic effect that “forbids” low rigidity cosmic rays from reaching the vicinity of the Earth. If one neglects the effects of the geomagnetic field on the shower development it is possible to “translate” a shower from a position on the Earth to an arbitrary one, keeping the zenith angle of the primary particle (and therefore the zenith angle of all particles) as constant (this of course corresponds to a rotation of a shower seen as “rigid body” around the center of the Earth, plus an additional rotation around the new vertical axis). A single shower generated by montecarlo can then be “used” many times

with enormous saving of computer time. The effects of the geomagnetic effects in the determination of the allowed and forbidden trajectories can be easily included, checking that if a given shower position corresponds to an allowed or forbidden primary trajectory and rejecting forbidden trajectories. A preliminary calculation using this method for the three sites of Kamioka, Soudan and Gran Sasso has been recently made available on the web by Battistoni et al. [26].

6.3 Weighted technique

If the effects of the magnetic fields are also included in the development of the shower, the problem loses all symmetry and one has to confront the computational problem of a calculation that is intrinsically very inefficient. A solution of this problem that is under study [27], is to use a weighted technique, generating the cosmic ray showers with a strong bias in position and direction, so that the neutrinos produced are more likely to arrive in the vicinity of the detector in consideration, and using a weight system to estimate correctly the flux. In this method approximately half of the cosmic rays interact in a small region above the detector to simulate the down-going flux, while approximately one half are generated over the rest of the Earth's surface. For these events the direction of the shower is chosen preferentially in a cone with an axis that "points" toward the detector. In this way it is possible to collect a sufficiently large statistics of neutrinos in a relatively small area around the detector site.

6.4 Direct approach

A possible solution is also to neglect any attempt at simplification, or optimization, and simply generate all cosmic showers on the Earth with a realistic distributions in position and direction, that only takes into account the geomagnetic effects studying the development of the showers in a realistic magnetic field. Such a calculation will produce a population of neutrinos that is distributed quasi-uniformly over the entire surface of the Earth, with the non-uniformities representing the expected variations in intensity due to geomagnetic effects, that produce a larger (smaller) flux in the magnetic polar (equatorial) region. In this direct (or brute force) approach the calculation is not performed for a given detector position, because all positions on the Earth are treated "democratically". This is the technique used in [17] and also in this work. Its only drawback is that the results that can be obtained in a reasonable time integrating then neutrino results over a large area of the Earth.

References

- [1] Super-Kamiokande collaboration, Y. Fukuda et al Phys.Rev.Lett. 81, 1562 (1998).
- [2] Kamiokande collaboration, K.S. Hirata et al, Phys. Lett. B 205, 416 (1988); Phys. Lett. B 280, 146 (1992); Y. Fukuda *et al*, Phys. Lett. B 335, 237 (1994).
- [3] IMB collaboration, D. Casper et al, Phys. Rev. Lett. 66, 2561 (1991); R. Becker-Szendy *et al*, Phys. Rev. D 46, 3720 (1992).
- [4] Soudan collaboration, W. W. M. Allison *et al.*, Phys. Lett. B449, 137 (1999).
- [5] MACRO collaboration, Phys. Lett. B 434, 451 (1998) Preprint hep-ex/0001044 submitted to Phys.Lett. B (2000).
- [6] T. H. Johnson, Phys. Rev. 43, 307 (1933); 43, 381 (1933); 48, 287 (1935); see also B. Rossi, Cosmic Rays (McGraw-Hill, New York, 1964), and references therein.
- [7] L.W. Alvarez & A.H. Compton, Phys. Rev. 43, 835 (1933).
- [8] Super-Kamiokande collaboration, T. Futagami *et al.*, Phys.Rev.Lett. 82, 5194 (1999).
- [9] M. Honda, T. Kajita, K. Kasahara & S. Midorikawa, Phys. Rev. D 52 (1995) 4985.
- [10] P.Lipari, T. K. Gaisser and T. Stanev, Phys. Rev. D 58, 073003 (1998).
- [11] G. Battistoni, A. Ferrari, P. Lipari, T. Montaruli, P. R. Sala and T. Rancati, Astroparticle Physics 12, 315 (2000), also available as hep-ph/9907408.
- [12] G. Lemaître and M.S. Vallarta, Phys. Rev. 43, 87, (1933).
- [13] The International Geomagnetic Reference Field (IGRF) is available with regular updates at: <http://nssdc.gsfc.nasa.gov/space/model/magnetos/igrf.html>
- [14] C. Störmer, Astrophysics 1, 237 (1930).
- [15] H.M.Hillas, in Proc.17th Int.Cosmic Ray Conf. (Paris) 8, 193, (1981). The model is also discussed in T . K. Gaisser, “Cosmic Rays and Particle Physics”, Cambridge University Press, (1990).
- [16] P. Lipari, M. Lusignoli and F. Sartogo. Phys.Rev.Lett. 74, 4384 (1995).
- [17] Paolo Lipari, hep-ph/0002282 (2000).
- [18] Vivek Agrawal, T.K. Gaisser, Paolo Lipari & Todor Stanev, Phys. Rev. D 53, 1314 (1996).
- [19] Private communications with T.K. Gaisser, T. Stanev, M. Honda, K. Kasahara, G. Battistoni, A. Ferrari and others.
- [20] Paolo Lipari, in Proceedings of the 8th International Workshop on ”Neutrino Telescopes”. (edited by Milla Baldo Ceolin); available as hep-ph/9905506.

- [21] T.K. Gaisser. in Proceedings of TAUP99; available as hep-ph/0001027.
- [22] Caprice collaboration, M. Boezio *et al.*, Ap.J. 518, 457 (1999).
- [23] AMS collaboration, Phys. Lett. B 472, 215 (2000).
- [24] BESS collaboration, T. Sanuki *et al.*, astro-ph/0002481
- [25] See for example the HARP proposal: cern-spsc/99.35
- [26] See the URL <http://www.mi.infn.it/~battist/neutrino.html>
- [27] Giuseppe Battistoni and Alfredo Ferrari private communication.

Region: $\sin \lambda_{\text{mag}} = [-0.2, +0.2]$

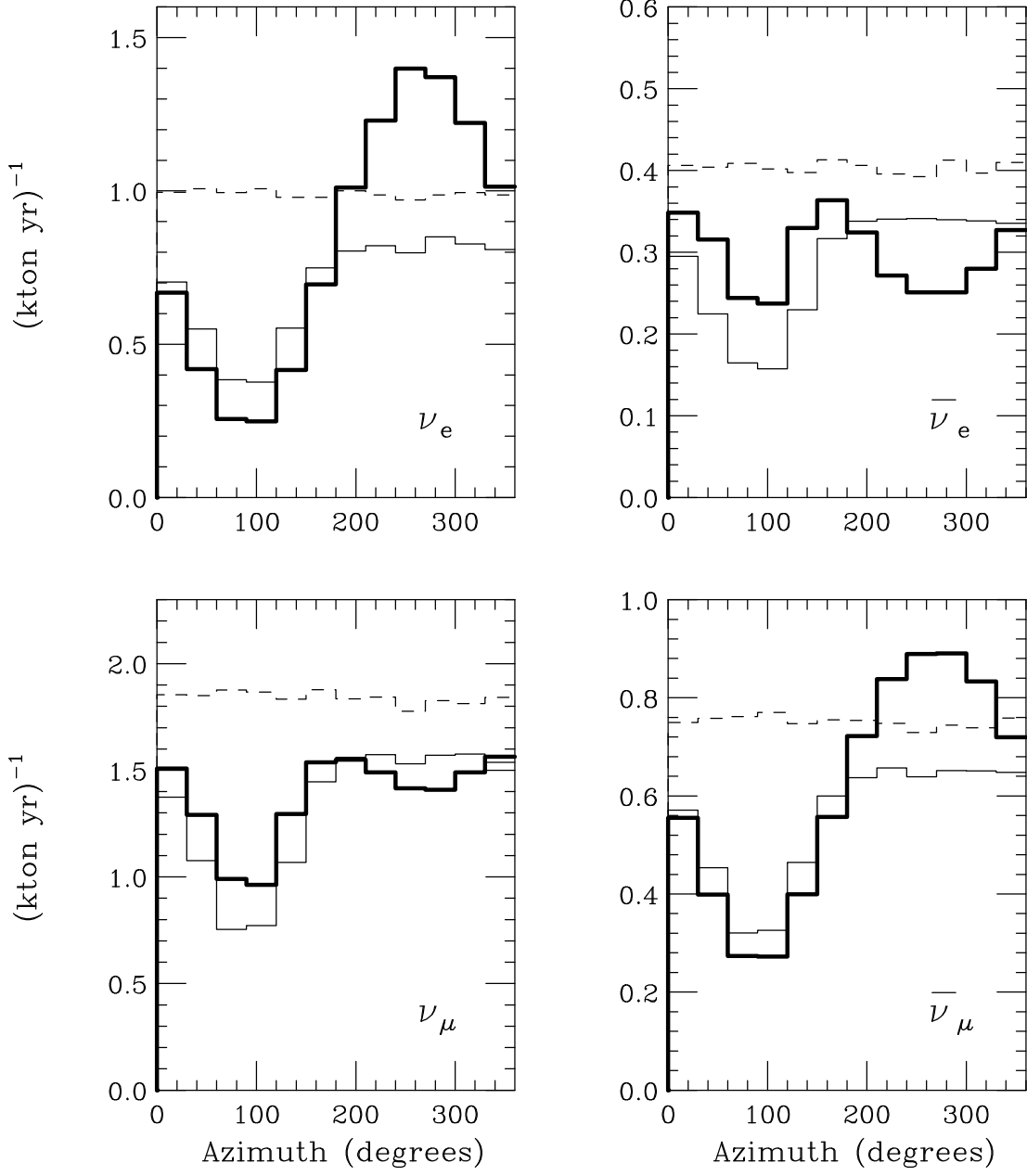


Figure 3: Azimuth angle distributions of atmospheric neutrino events. The distributions are averaged for detectors uniformly distributed on all positions in the Earth magnetic equatorial region ($\sin \lambda_M = [-0.2, 0.2]$). The four panel are for neutrinos of different type. The three histograms are for: fully 3-D calculation (thick), 1-D calculation (thin), 1-D without geomagnetic effects (dashed).

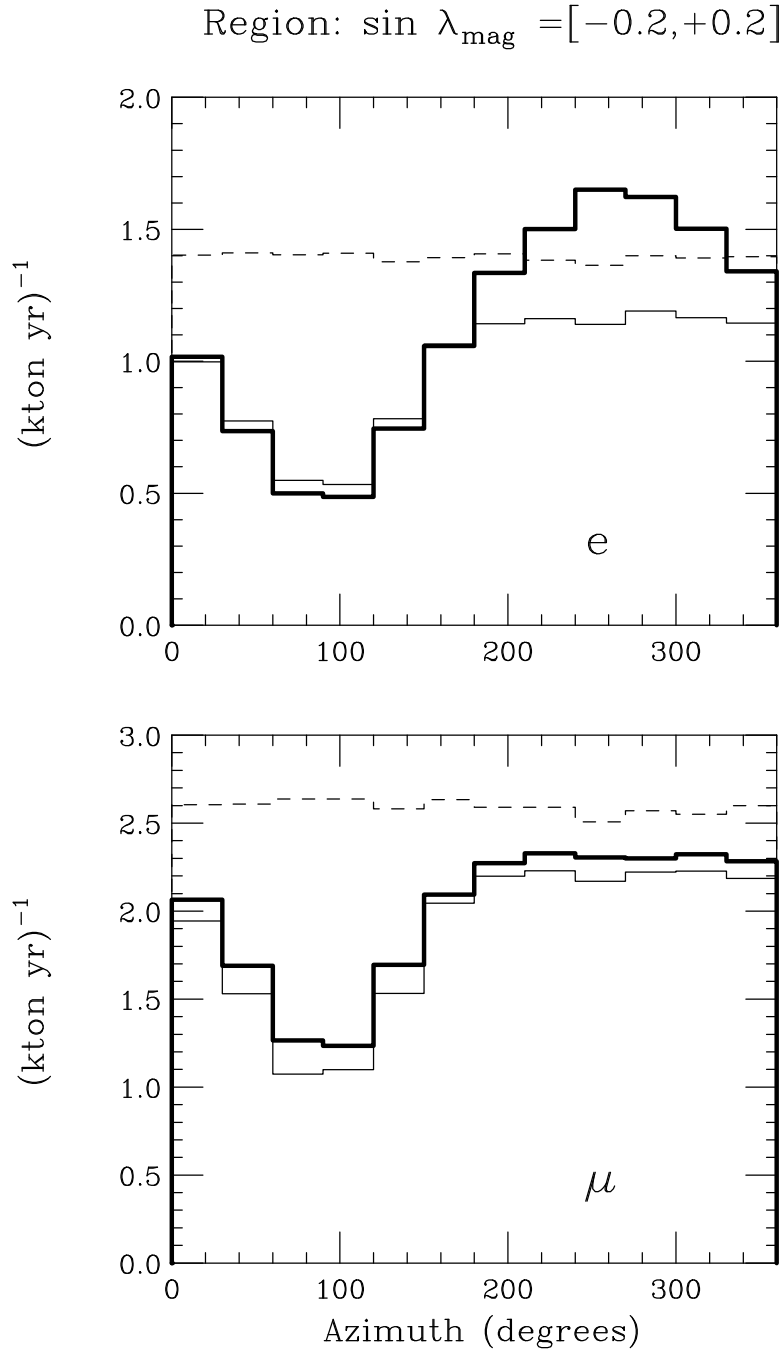


Figure 4: Azimuth angle distributions of atmospheric neutrino events. The distributions are averaged for detectors uniformly distributed on all positions in the Earth magnetic equatorial region ($\sin \lambda_M = [-0.2, 0.2]$). The upper (lower) panel is for e -like (μ -like) events. The three histograms are for: fully 3-D calculation (thick), 1-D calculation (thin), 1-D without geomagnetic effects (dashed).

Region: $\sin \lambda_{\text{mag}} = [0.2, 0.6]$

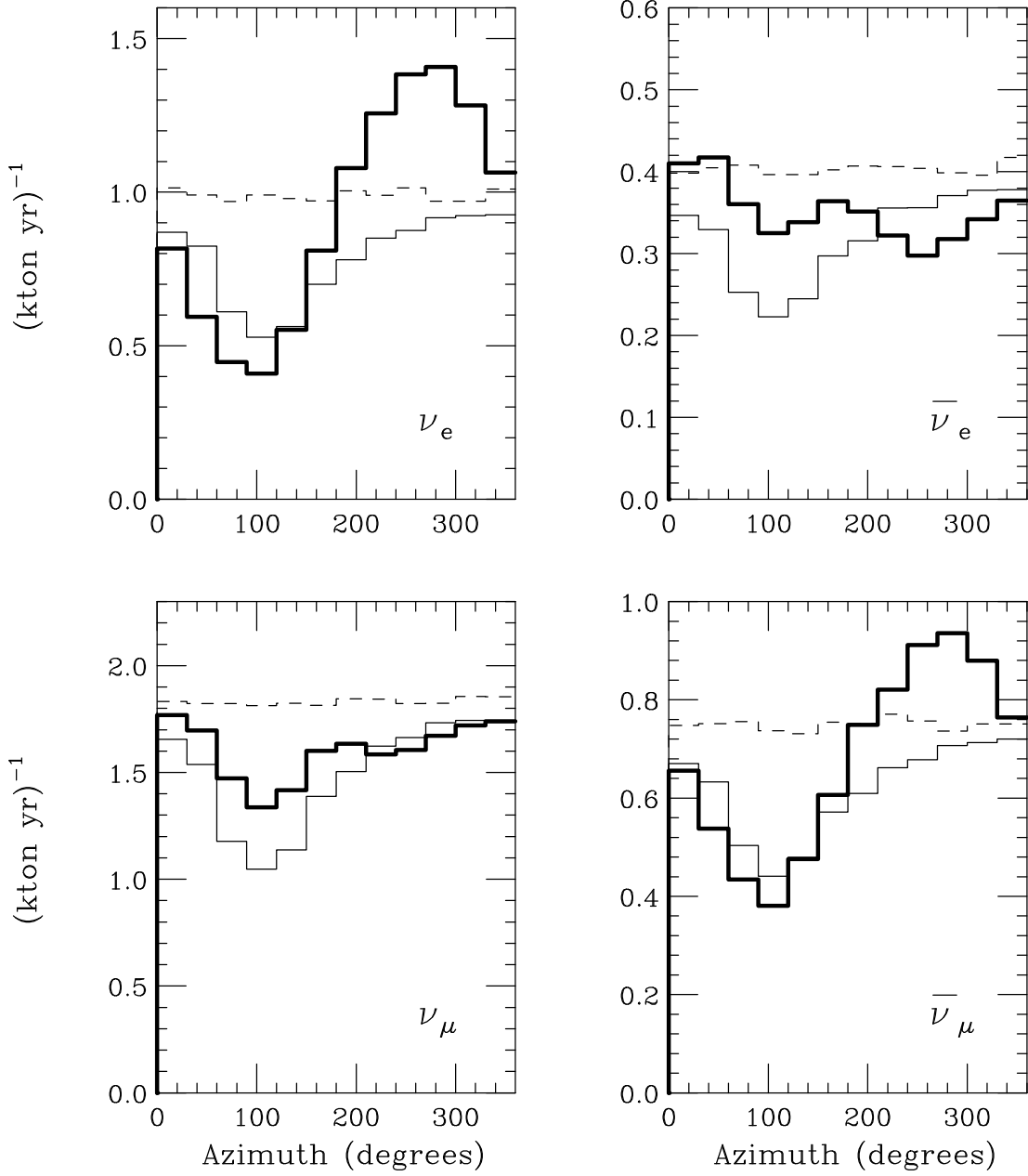


Figure 5: Azimuth angle distributions of atmospheric neutrino events. The distributions are averaged for detectors uniformly distributed on all positions on the Earth with magnetic latitude $\sin \lambda_M = [0.2, 0.6]$. (The SK detector has magnetic latitude $\sin \lambda_M^{\text{SK}} = 0.455$) The four panel are for neutrinos of different type. The three histograms are for: fully 3-D calculation (thick), 1-D calculation (thin), 1-D without geomagnetic effects (dashed).

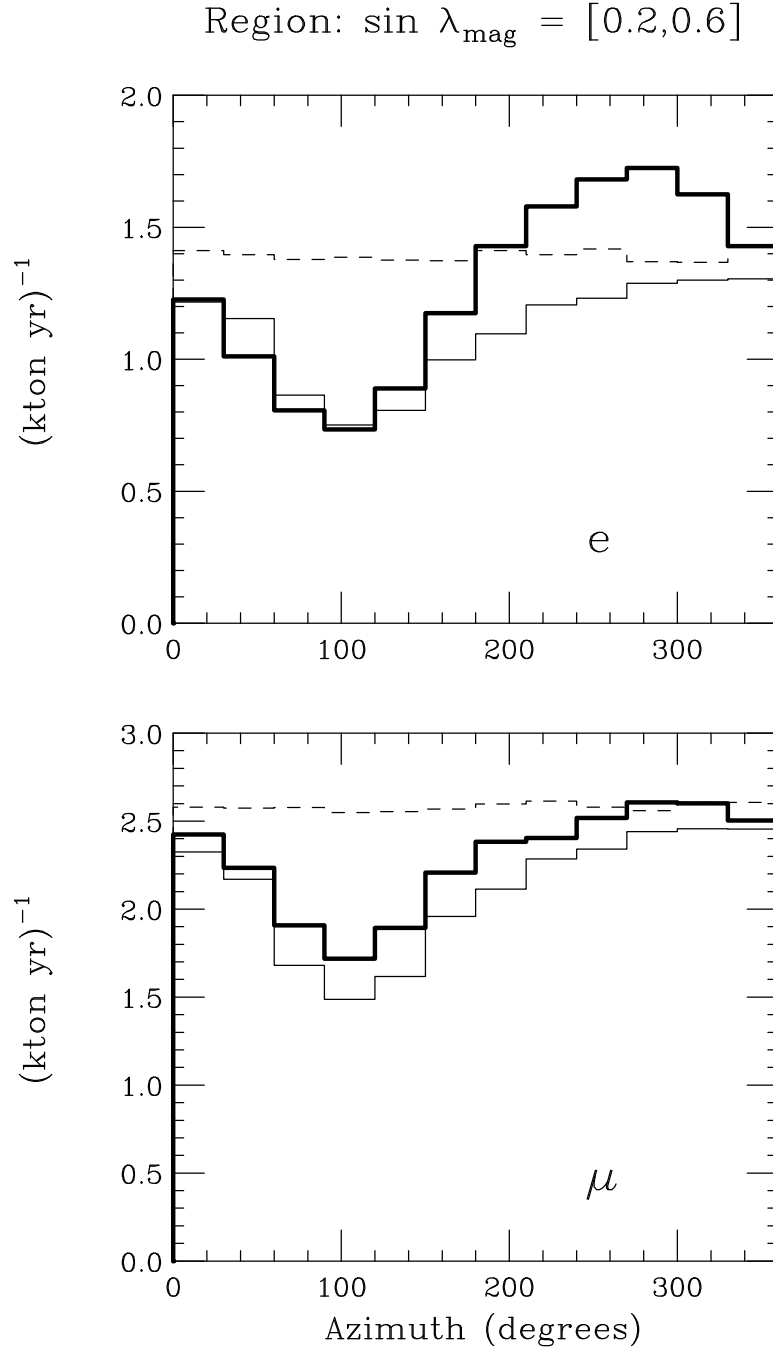


Figure 6: Azimuth angle distributions of atmospheric neutrino events. The distributions are averaged for detectors uniformly distributed on all positions on the Earth with magnetic latitude $\sin \lambda_M = [0.2, 0.6]$. (The SK detector has magnetic latitude $\sin \lambda_M^{\text{SK}} = 0.455$) The upper (lower) panel is for e -like (μ -like) events. The three histograms are for: fully 3-D calculation (thick), 1-D calculation (thin), 1-D without geomagnetic effects (dashed).

Region: $\sin \lambda_{\text{mag}} = [0.6, 1]$

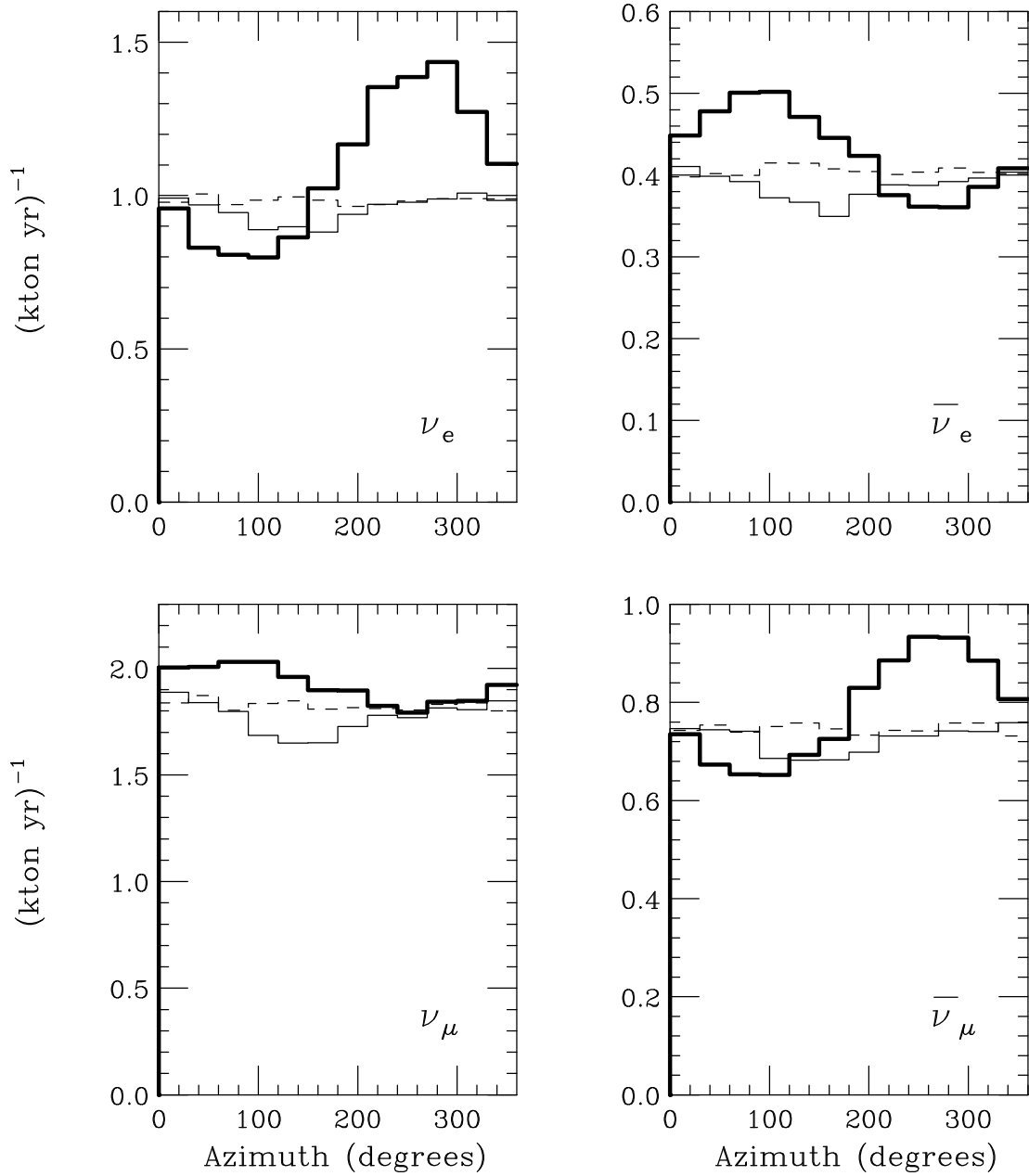


Figure 7: Azimuth angle distributions of atmospheric neutrino events. The distributions are averaged for detectors uniformly distributed on all positions in the Earth magnetic north polar region ($\sin \lambda_M = [0.6, 1]$). The four panel are for neutrinos of different type. The three histograms are for: fully 3-D calculation (thick), 1-D calculation (thin), 1-D without geomagnetic effects (dashed).

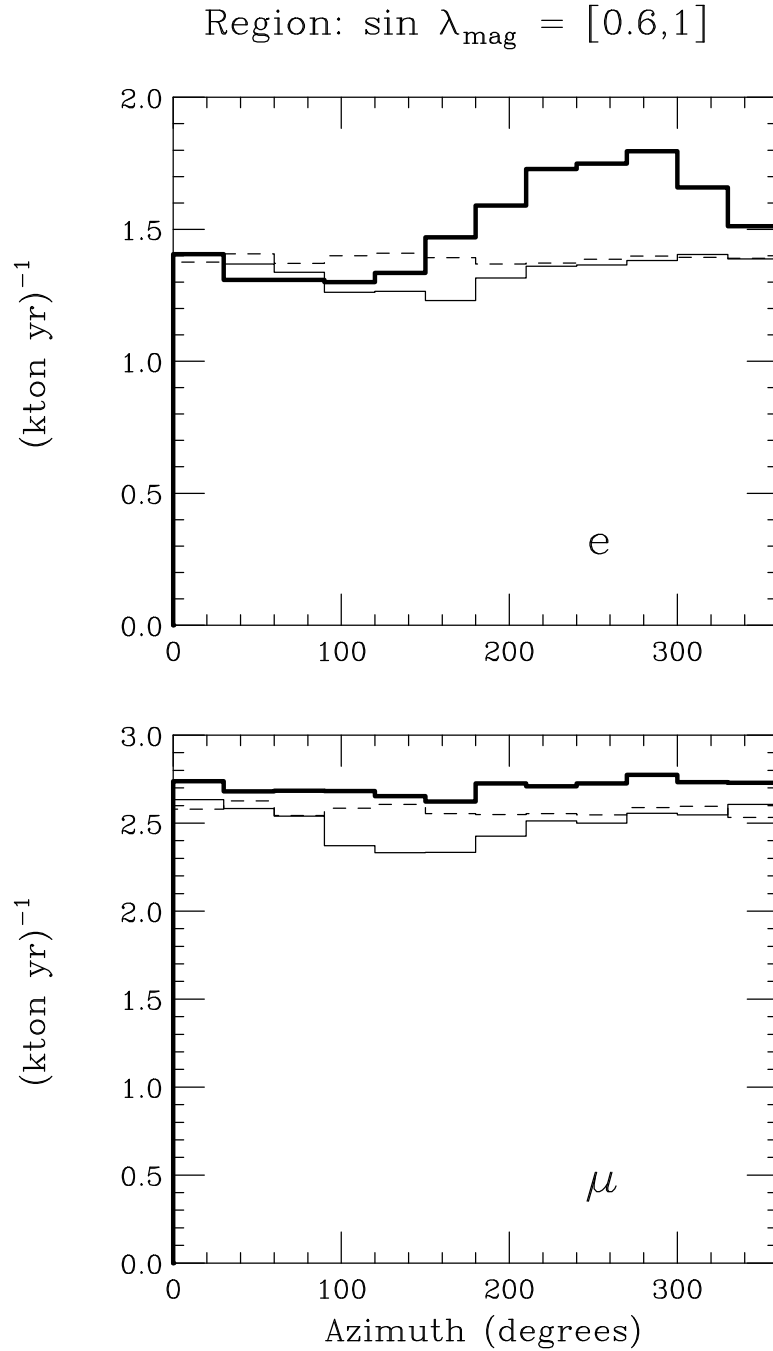


Figure 8: Azimuth angle distributions of atmospheric neutrino events. The distributions are averaged for detectors uniformly distributed on all positions in the Earth magnetic north polar region ($\sin \lambda_M = [0.6, 1]$). The upper (lower) panel is for e -like (μ -like) events. The three histograms are for: fully 3-D calculation (thick), 1-D calculation (thin), 1-D without geomagnetic effects (dashed).